Stochastic resonance of abundance fluctuations and mean time to extinction in an ecological community

Jong Il Park [1], Beom Jun Kim,[1] and Hye Jin Park [2,3,*]

[1]*Department of Physics, Sungkyunkwan University, Suwon 16419, Republic of Korea*

[2]*Asia Pacific Center for Theoretical Physics, Pohang 37673, Republic of Korea*

[3]*Department of Physics, POSTECH, Pohang 37673, Republic of Korea*

(Received 4 March 2021; accepted 11 August 2021; published 26 August 2021)

Periodic environmental changes are commonly observed in nature from the amount of daylight to seasonal temperature. These changes usually affect individuals' death or birth rates, dragging the system from its previous stable states. When the fluctuation of abundance is amplified due to such changes, extinction of species may be accelerated. To see this effect, we examine how the abundance and the mean time to extinction respond to the periodic environmental changes. We consider a population wherein two species coexist together implemented by three rules—birth, spontaneous death, and death from competitions. As the interspecific interaction strength is varied, we observe the resonance behavior in both fluctuations of abundances and the mean time to extinction. Our result suggests that neither too high nor too low competition rates make the system more susceptible to environmental changes.

DOI: 10.1103/PhysRevE.104.024133

I. INTRODUCTION

Temporal environmental variations commonly occur in ecosystems through the variations of sunlight, atmospheric circulation, precipitation, etc. Those variations are often periodic because the variations mainly come from the revolution and rotation of the Earth, alternating the evolutionary favorable species in an ecological community. For example, two barnacle species favors different temperature competing for free space in intertidal zone, *Semibalanus balanoides* and *Chthamalus*: the former outperforms in arctic-boreal region while the latter favors warm water. As two species have different thermal tolerances, it has been reported that sea surface temperature (SST) determines which species will successfully take over free space; the rise of SST makes *S. balanoides* exclude *Chthamalus* by occupying free space, and vice versa with temperature drop [1–3]. Likewise, seasonal temperature changes induce the variation of interspecific interactions, eventually leads to the fluctuation of abundances. Thus, environmental variations may destabilize the coexistence and can even cause the extinction of one species.

Effects of such alternating environmental changes on ecological communities have recently received increasing attention [4–7] while most existing studies focused on a constant environment. For example, it has been shown that switching environments can exponentially reduce the mean time to extinction (MTE) of a single-species population described by simple birth-death processes [4]. Besides extinction behavior, a stationary abundance distribution under switching environments has been investigated for a single-species population as well [5]. For two-species populations, analytical tools to study the extinction behavior have been recently developed in Refs. [6,7]. Those studies have well explained the role of environmental variations in shaping ecological communities. However, studies on stochastic resonance (SR) behavior related to the environmental changes are still lacking. Even though SR has been observed for a single-type population with bistable states [8], yet the underlying mechanism has not been related to the environmental variations.

Stochastic resonance is a phenomenon in that noise can amplify a response signal when a system confronts an energy barrier under a periodic external driving force [9]. It occurs when the internal timescale of the system determined by noise matches the timescale of an external signal [9–13]. When it comes to a dynamical system, the internal timescale can be determined by how fast the system relaxes toward a stable fixed point, which is related to the curvature of the corresponding Lyapunov function. Thus Lyapunov function of the abundance dynamics is analogous to free-energy landscape determining the intrinsic timescale of the system. Even though there are no explicit noise and energy barriers in ecological systems described by birth and death processes, from the above analogy we can expect that SR behavior may occur in the dynamical system with environmental variation which acts as an external field.

Our main goal is to detect the SR in a two-species system that has a single coexistence state, which maps into a stochastic competitive Lotka-Volterra model [14–17]. Specifically, to explore how periodic environmental changes affect an ecological system we design the three reaction rules for population dynamics: birth, spontaneous death, and competition death. Brought from the evolutionary game analogy, we connect payoffs and the competition death rates. We implement the temporal environmental changes which are alternating

*hyejin.park@apctp.org

favorable species by time-varying interspecific interactions. To capture SR behavior, we estimate how the system responds to the environmental changes within the linear response theory scheme.

To examine the behavior of abundance fluctuations and the MTE, we use both deterministic and stochastic approaches. The deterministic approach well describes the average abundances, providing well-known equations called the competitive Lotka-Volterra equations [18,19]. A master equation is used to deal with probabilities for considering extinction behavior caused by noise. We define two different susceptibilities for each approach and check the SR behavior via the existence of susceptibility peaks.

This paper is organized as follows. In Sec. II, we introduce the birth and death rules which describe ecological systems with temporal environmental changes. Assuming infinitesimally small environmental changes, we analytically investigate how the abundance fluctuations and the MTE respond in Secs. III and IV, respectively. Finally, we summarize our findings and discuss them in Sec. V.

II. MODEL

We consider a two-species population using an individual-based model. Each individual gives birth and spontaneously dies with constant rates λ_b and λ_d, respectively. Competition occurs between any two individuals, and one of them dies at a certain rate. We assume that birth and spontaneous death rates are the same for both species, while the competition death rates depend on the species of competing individuals. In summary, all three rules governing population dynamics are represented by the following reaction scheme:

$$\begin{aligned} X_i &\to X_i + X_i \qquad \text{at rate } \lambda_b, \\ X_i &\to \emptyset \qquad\quad \text{at rate } \lambda_d, \\ X_i + X_j &\to X_j \qquad \text{at rate } \alpha_{ij}, \end{aligned} \tag{1}$$

where X_i and X_j indicate individuals of species i and j, respectively ($i, j \in \{1, 2\}$). When the net growth rate without competition is positive ($\lambda_b > \lambda_d$), the population is regulated by the competition death, having a steady state.

Connecting the competition death rates to payoffs in evolutionary game theory [16,20], we set the competition death rate as a decreasing function of the payoff $\Lambda_{ij} (> 0)$:

$$\alpha_{ij} = (M\Lambda_{ij})^{-1}. \tag{2}$$

The parameter M scales the strength of competition rates determining the magnitude of the population size. The formula indicates that an individual who has a huge payoff is less likely to die.

For the sake of simplicity, we consider the symmetric payoff matrix

$$\mathbf{\Lambda} = \begin{bmatrix} a & b \\ b & a \end{bmatrix}. \tag{3}$$

The diagonal elements of $\mathbf{\Lambda}$ represent the payoff of intraspecific interactions and off-diagonal elements represent the payoff of interspecific interactions. There is no competition advantage bias for any species, but the competition death rates depend on interaction types. To guarantee the coexistence of two species, we focus on the case where the interspecific interaction gives a higher payoff than the intraspecific interaction ($a < b$) [16].

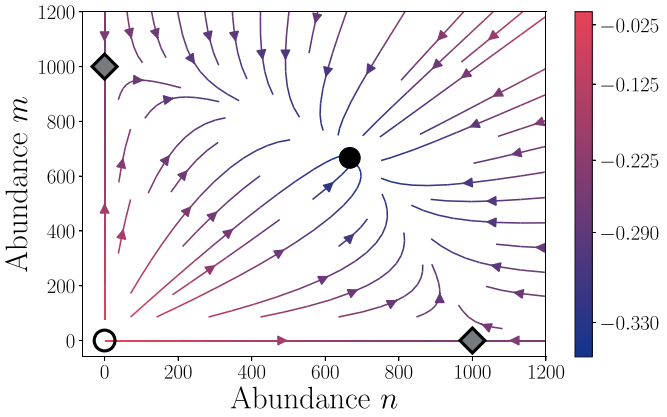

FIG. 1. Abundance dynamics and the fixed points of Eq. (5) without an external field. Four symbols represent the fixed points: the open circle (unstable), two gray-filled diamonds (saddle), and the black-filled circle (stable). The color of the arrows indicate the values of the Lyapunov function, $\phi(n, m) = \frac{\mu}{2M^2}(n^2 + m^2) - \frac{\lambda\mu}{M}(n + m) + \frac{nm}{M^2}$ (see Appendix A). The coexistence is the only stable fixed point located at the minimum of the Lyapunov function. Parameters $M = 2000$, $\lambda_b = 0.6$, $\lambda_d = 0.1$, and $\mu = 2$ are used.

Now we take the periodic environmental changes into account through modulating the interspecific payoff in time. We also normalize the payoff matrix with a without loss of generality. Thus, the time-varying payoff matrix becomes

$$\mathbf{\Lambda}(t) = \begin{bmatrix} 1 & \mu + \epsilon \sin \omega t \\ \mu - \epsilon \sin \omega t & 1 \end{bmatrix}. \tag{4}$$

Different species have opposite effects (competition advantage or disadvantage) from the environment. The criterion for the coexistence of two species is $1 < \mu - \epsilon$. Hereafter, we treat the environmental changes as an "external field," and ϵ and ω are the amplitude and the angular frequency of the external field. Considering infinitesimally small external field $\epsilon \ll 1$, we investigate how the system responds to the external field.

III. STOCHASTIC RESONANCE OF ABUNDANCE FLUCTUATIONS

To investigate the abundance fluctuation induced by the temporal environmental changes, we focus on the abundance dynamics. For large population sizes (equivalently for large M values), the abundances n and m of each species 1 and 2 can be described by the deterministic equations,

$$\begin{aligned} \dot{n} &= n\left[\lambda - \frac{1}{M}\left(n + \frac{m}{\mu + h(t)}\right)\right], \\ \dot{m} &= m\left[\lambda - \frac{1}{M}\left(\frac{n}{\mu - h(t)} + m\right)\right], \end{aligned} \tag{5}$$

where $h(t) \equiv \epsilon \sin \omega t$ and $\lambda \equiv \lambda_b - \lambda_d$. With the adiabatic approximation ($\omega \ll 1$), we can find four fixed points for this system: (0,0), (λM, 0), (0, λM), and ($n^*(t)$, $m^*(t)$). Under the coexistence criterion, only the coexistence fixed point

$[n^*(t), m^*(t)]$ is stable; (0,0) is unstable; $(\lambda M, 0)$ and $(0, \lambda M)$ are saddle fixed points. The fixed points and the dynamic flows of Eq. (5) without an external field ($h = 0$) are shown in Fig. 1. The position of the stable fixed point $(n^*(t), m^*(t))$ varies in time with a nonzero field $h(t)$,

$$n^*(t) = \frac{(\mu - h)(\mu + h - 1)}{\mu^2 - h^2 - 1}\lambda M,$$
$$m^*(t) = \frac{(\mu + h)(\mu - h - 1)}{\mu^2 - h^2 - 1}\lambda M. \tag{6}$$

This indicates that the abundances fluctuate due to the external field $h(t)$.

Considering the normalized abundances $x = n/M$ and $y = m/M$, we get rid of M dependency in the dynamics [dividing Eq. (5) by M and writing them in terms of x and y]. Thus the normalized abundances follow the trajectory of $[x^*(t), y^*(t)]$. When the environmental changes are sufficiently small ($\mu \gg \epsilon$), the system will fluctuate around the zero-field ($h = 0$) coexistence state $(x^*, y^*) = (\frac{\mu\lambda}{\mu+1}, \frac{\mu\lambda}{\mu+1})$. The dynamics of normalized abundance fluctuation $\boldsymbol{\delta} = (\delta_x, \delta_y)$ is then

$$\dot{\delta}_x = \frac{\lambda^2}{(\mu+1)^2}h - \frac{\lambda\mu}{\mu+1}\delta_x - \frac{\lambda}{\mu+1}\delta_y + O(\delta^2, h\delta),$$
$$\dot{\delta}_y = -\frac{\lambda^2}{(\mu+1)^2}h - \frac{\lambda}{\mu+1}\delta_x - \frac{\lambda\mu}{\mu+1}\delta_y + O(\delta^2, h\delta). \tag{7}$$

These fluctuations capture the averaged noise behavior, allowing us to examine the stochastic effect (see Appendix B).

Because of interspecific interactions, the dynamics of δ_x and δ_y are coupled. By setting new variables, $\delta_\parallel = (\delta_x - \delta_y)/\sqrt{2}$ and $\delta_\perp = (\delta_x + \delta_y)/\sqrt{2}$, we can decouple the dynamics,

$$\dot{\delta}_\parallel = \sqrt{2}h_\parallel - \frac{\mu - 1}{\mu + 1}\lambda\delta_\parallel,$$
$$\dot{\delta}_\perp = -\lambda\delta_\perp, \tag{8}$$

with the external field $h_\parallel \equiv [\lambda^2/(\mu+1)^2]h$ for the $\delta_\parallel$ direction. For the zero-field case, both parallel ($\parallel$) and perpendicular ($\perp$) fluctuations decay exponentially. The relaxation times are $\tau_\parallel^{-1} = \lambda(\mu - 1)/(\mu + 1)$ and $\tau_\perp^{-1} = \lambda$, respectively.

However, with the time-varying external field, only the perpendicular direction has an exponentially decaying solution, not the parallel direction. Thus, after a transient time, the system fluctuates only in the parallel direction, effectively reducing its dynamics into the one-dimensional behavior. Solving Eq. (8), we obtain the oscillating fluctuation in the parallel direction,

$$\delta_\parallel(t) = \delta_0 \sin(\omega t - \sigma), \tag{9}$$

with the phase lag $\sigma = \tan^{-1}(\omega\tau_\parallel)$ and the amplitude

$$\delta_0 = \frac{\sqrt{2}\lambda^2}{(\mu+1)^2}\frac{\epsilon\tau_\parallel}{\sqrt{1 + \omega^2\tau_\parallel^2}}. \tag{10}$$

The fluctuation amplitude δ_0 is maximized at $\omega = 0$, which means that there is no classical resonance behavior for this system; see Fig. 2(a). It is because the system is described by the first-order ordinary differential equations (ODEs).

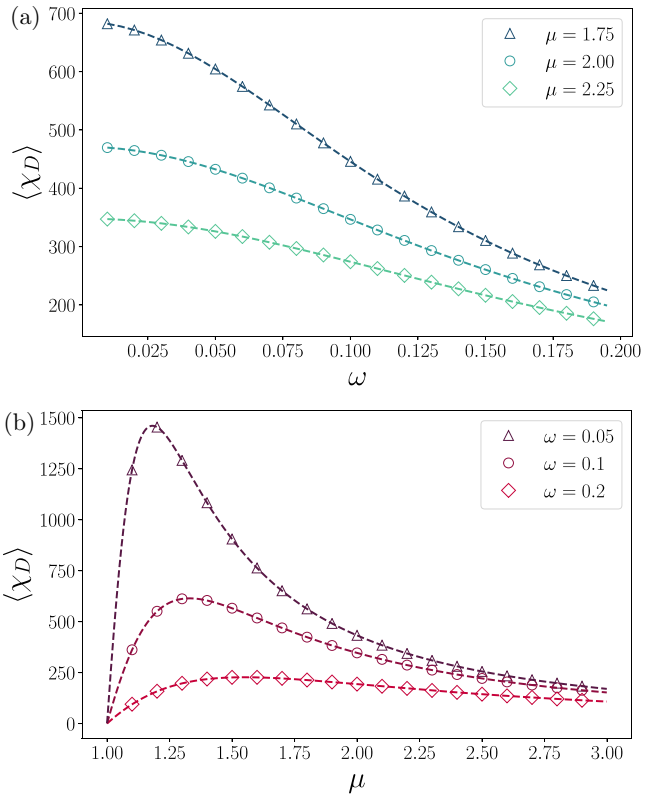

FIG. 2. The time-averaged susceptibility $\langle \chi_D \rangle$ is plotted with respect to (a) ω for $\mu = 1.75$, 2.00, and 2.25; (b) μ for $\omega = 0.05$, 0.1, and 0.2. The dashed lines and symbols in (a) and (b) indicate theoretical and numerical results, respectively, exhibiting very good agreement. The time average has been taken within the last 20 periods to avoid transient behavior within the whole 1000 periods of simulation. For numerical calculations, we used the improved Euler method with $M = 2000$, $\lambda_b = 0.6$, $\lambda_d = 0.1$, and $\epsilon = 0.01$.

While the parameters λ and M merely scale the Lyapunov function, the interspecific interaction μ changes the functional shape (see Appendix A). Regarding the Lyapunov function as a free-energy landscape, the role of interspecific interaction payoff μ is analogous to "temperature" [12]. Thus, we expect that SR occurs by varying μ: abundance fluctuation induced by an external field is maximized at a certain μ value. There still exists a debate on the use of the term *stochastic resonance* for results obtained from a deterministic equation. However, we keep the widely used terminology because the abundance fluctuations we obtained capture the averaged noise dynamics. To see the SR behavior, we use linear response theory,

$$N_\parallel(t) = \int_{-\infty}^{\infty} \frac{\delta N_\parallel(t)}{\delta h(t')} h(t')\, dt'. \tag{11}$$

Inserting $N_\parallel(t) = M\delta_\parallel(t)$ and taking Fourier transform, we can measure how susceptible the system is to the external driving field through the use of the so-called susceptibility given by

$$\chi_D(\omega, \mu) = \mathrm{Re}\left[\lim_{\delta h \to 0} \frac{\delta N_\parallel(\omega)}{\delta h(\omega)}\right] = \frac{\sqrt{2}\lambda^2 M}{(\mu+1)^2}\frac{\tau_\parallel}{1 + \omega^2\tau_\parallel^2}. \tag{12}$$

Since $\chi_D \to 0$ for both limiting cases of $\mu \to 1$ and $\mu \to \infty$, χ_D is maximized when $\partial\chi_D/\partial\mu = 0$. From

$$\frac{\partial\chi_D}{\partial\mu} = \chi_D\left[1 + 2\tau_\parallel\left(\frac{1}{\lambda\tau_\parallel^2 - \tau_\parallel} - \frac{\omega^2\tau_\parallel}{1+\omega^2\tau_\parallel^2}\right)\right]\frac{d\tau_\parallel}{d\mu}, \quad (13)$$

the extremum condition yields a solution $\mu = \mu_D$ which satisfies the equivalent condition $\omega = \tau_\parallel^{-1}\sqrt{(\lambda\tau_\parallel+1)/(\lambda\tau_\parallel-3)}$. Thus, the resonance occurs at μ_D where $\omega = \tau_\parallel^{-1}$ is satisfied for $\lambda\tau_\parallel \gg 1$. This theoretical prediction agrees well with numerical calculations of solving Eq. (5); see Fig. 2(b).

IV. STOCHASTIC RESONANCE OF MEAN TIME TO EXTINCTION

Since the abundance fluctuation is amplified at a certain μ value, we expect that such SR behavior occurs for the mean time to extinction (MTE) as well. Hence, in this section, we examine how the environmental changes affect the extinction time. Because the deterministic approach cannot capture the extinction behavior, we deal with a stochastic approach. Starting from a master equation, a set of time differential equations of probabilities for each abundance state, we will calculate the MTE by using Wentzel-Kramers-Brillouin (WKB) approximation [8,21–25].

Without the field, the probability distribution $P_{n,m}(t)$ for the system to be in state (n, m) at time t follows the master equation,

$$\begin{aligned}\dot{P}_{n,m} &= \lambda_b[(n-1)P_{n-1,m}+(m-1)P_{n,m-1}-(n+m)P_{n,m}]\\ &+\lambda_d[(n+1)P_{n+1,m}+(m+1)P_{n,m+1}-(n+m)P_{n,m}]\\ &+\frac{1}{M}[(n+1)nP_{n+1,m}+(m+1)mP_{n,m+1}\\ &-n(n-1)P_{n,m}-m(m-1)P_{n,m}]\\ &+\frac{1}{\mu M}[(n+1)mP_{n+1,m}+n(m+1)P_{n,m+1}-2nmP_{n,m}].\end{aligned} \quad (14)$$

Introducing a generating function

$$G(p_1, p_2, t) = \sum_{n,m} p_1^n p_2^m P_{n,m}(t), \quad (15)$$

we derive the effective Hamiltonian operator $\hat{H}_0$ from Eq. (14) [8,22,23,25]. The imaginary-time Schödinger equation scheme is applied, $\partial_t G = -\hat{H}_0 G$. The separable solution of momentum-space WKB ansatz is assumed as $G(p_1, p_2, t) = e^{-t/\tau}e^{-S_0(p_1,p_2)}$, where $1/\tau$ is an exponentially small eigenvalue of $\hat{H}_0$.

Neglecting the second-order derivatives of $S_0(p_1, p_2)$ with respect to p_1 and p_2 we obtain a classical Hamilton-Jacobi equation, $H_0 \approx 0$, with a Hamiltonian H_0,

$$\begin{aligned}H_0 &= \lambda_b[(1-p_1)p_1q_1 + (1-p_2)p_2q_2]\\ &+\lambda_d[(p_1-1)q_1 + (p_2-1)q_2]\\ &+\frac{1}{M}\left[(p_1-1)p_1q_1^2 + (p_2-1)p_2q_2^2\right]\\ &+\frac{1}{\mu M}[(p_1-1)p_2q_1q_2 + (p_2-1)p_1q_1q_2],\end{aligned} \quad (16)$$

with the conjugate coordinates defined as $q_1 \equiv -\partial_{p_1}S$ and $q_2 \equiv -\partial_{p_2}S$. The system is now mapped into four-dimensional phase space with corresponding equations of motion:

$$\begin{aligned}\dot{q}_1 &= -\partial_{p_1}H_0 = \lambda_b(2p_1-1)q_1 - \lambda_d q_1 - \frac{1}{M}(2p_1-1)q_1^2 - \frac{1}{\mu M}(2p_2-1)q_1q_2,\\ \dot{q}_2 &= -\partial_{p_2}H_0 = \lambda_b(2p_2-1)q_2 - \lambda_d q_2 - \frac{1}{M}(2p_2-1)q_2^2 - \frac{1}{\mu M}(2p_1-1)q_1q_2,\\ \dot{p}_1 &= \partial_{q_1}H_0 = \lambda_b(1-p_1)p_1 + \lambda_d(p_1-1) + \frac{2}{M}(p_1-1)p_1q_1 + \frac{1}{\mu M}(2p_1p_2 - p_1 - p_2)q_2,\\ \dot{p}_2 &= \partial_{q_2}H_0 = \lambda_b(1-p_2)p_2 + \lambda_d(p_2-1) + \frac{2}{M}(p_2-1)p_2q_2 + \frac{1}{\mu M}(2p_1p_2 - p_2 - p_1)q_1.\end{aligned} \quad (17)$$

Equation (5), which is obtained in the deterministic approach, can be reproduced for $p_1 = p_2 = 1$. As the dimensionality of the system increases from two to four, two additional saddle points appear with zero energy ($H_0 = 0$) related to the extinction states: $\boldsymbol{\eta}_1 = (q_1, q_2, p_1, p_2) = (0, \lambda M, \frac{\lambda+\mu\lambda_d}{\mu\lambda_b}, 1)$ and $\boldsymbol{\eta}_2 = (\lambda M, 0, 1, \frac{\lambda+\mu\lambda_d}{\mu\lambda_b})$ which are saddle points. As the coexistence fixed point $\boldsymbol{\eta}_c = (\frac{\mu}{\mu+1}\lambda M, \frac{\mu}{\mu+1}\lambda M, 1, 1)$ also becomes a saddle, the transition from the coexistence state $\boldsymbol{\eta}_c$ to the extinction state $\boldsymbol{\eta}_1$ or $\boldsymbol{\eta}_2$ is possible, which has been forbidden in the deterministic approach.

The extinction mainly occurs along the zero-energy heteroclinic orbit from $\boldsymbol{\eta}_c$ to either $\boldsymbol{\eta}_1$ or $\boldsymbol{\eta}_2$ [26,27]. We estimate the mean time τ_E to extinction using the action S_0 along the extinction trajectory, $\tau_E \propto \exp(S_0)$ with

$$\begin{aligned}S_0 &= \int_{-\infty}^{\infty} L_0(p_i, \dot{p}_i, t)\,dt = \int_{-\infty}^{\infty}\left(-\sum_i q_i\dot{p}_i - H_0\right)dt,\\ &= -\int_{-\infty}^{\infty}(q_1\dot{p}_1 + q_2\dot{p}_2)\,dt.\end{aligned} \quad (18)$$

Here, L_0 is the momentum-space Lagrangian of Eq. (17). Since both species behave in the same way, we can only focus on the extinction from $\boldsymbol{\eta}_c$ to $\boldsymbol{\eta}_1$.

To find the extinction trajectory, we apply Chernykh-Stepanov iteration method [28,29]. The momenta $p_1(t)$ and

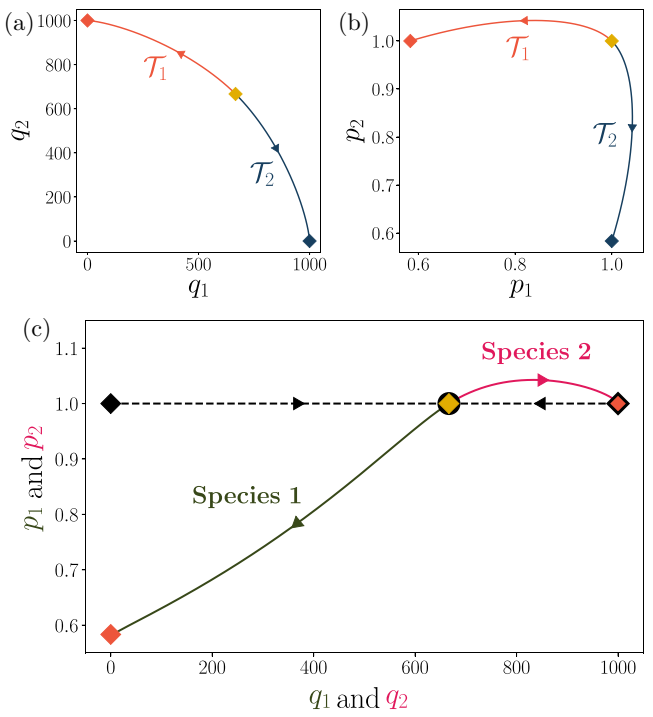

FIG. 3. The most probable extinction trajectory $\mathcal{T}_1(\mathcal{T}_2)$ from the coexistence state $\boldsymbol{\eta}_c$ to the extinction state $\boldsymbol{\eta}_1(\boldsymbol{\eta}_2)$ are projected on (a) coordinate and (b) momentum spaces. In panel (c), $\mathcal{T}_1$ is drawn in a phase space for each Species 1 (green) and Species 2 (pink). The dashed line is for the deterministic case, which is relevant to the case $p_1 = p_2 = 1$. Parameters $M = 2000$, $\lambda_b = 0.6$, $\lambda_d = 0.1$, and $\mu = 2$ are used.

$p_2(t)$ are obtained by solving Eq. (17) backward in time starting from momenta at $\boldsymbol{\eta}_1$. With these momenta, we obtain $q_1(t)$ and $q_2(t)$ by solving Eq. (17) forward in time with initial coordinates at $\boldsymbol{\eta}_c$. Again, the updated $q_1(t)$ and $q_2(t)$ are used for updating $p_1(t)$ and $q_2(t)$. We take this back-and-forth iteration process until the path converges to the heteroclinic orbit. The optimal path obtained by this numerical iteration is shown in Fig. 3. Calculating S_0 along the trajectory, we numerically get the mean time to extinction $\tau_E \propto \exp(S_0)$.

Now we consider the infinitesimal environmental changes $h(t)$. Because the magnitude of the external field is small enough, the new Hamiltonian H' can be written as $H' = H_0 + \epsilon H_p$ with

$$H_p(t, t_0) = \frac{\sin\omega(t - t_0)}{\mu^2 M}(p_2 - p_1)q_1 q_2. \tag{19}$$

Assuming the perturbed Hamiltonian ϵH_p is too small to affect the extinction trajectory obtained from the zero-field Hamiltonian, we calculate the minimum additional action along the same trajectory,

$$S_p = \min_{t_0}\left\{-\int_{-\infty}^{\infty} H_p(t, t_0)\, dt\right\}. \tag{20}$$

By varying the phase difference $t_0 \in (0, 2\pi]$, we numerically obtain the minimum additional action S_p with respect to t_0. The action S from $\boldsymbol{\eta}_c$ to $\boldsymbol{\eta}_1$ is now $S = S_0 + \epsilon S_p$, which leads to the estimation of MTE by $\tau_E \propto \exp(S_0 + \epsilon S_p)$. Thus

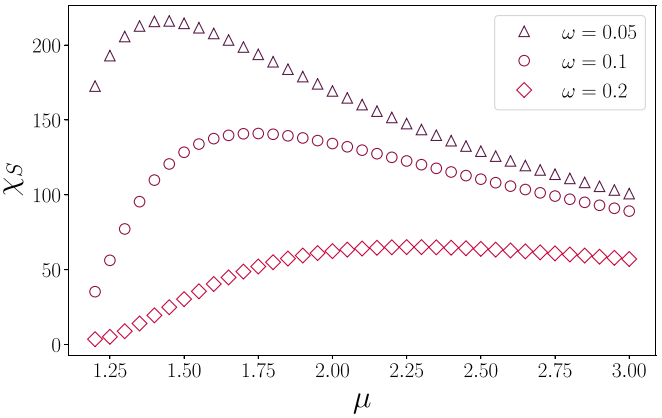

FIG. 4. The logarithmic susceptibility χ_S is plotted with respect to μ for $\omega = 0.05,\ 0.1,\ 0.2$. In each ω value, we can observe a single peak of χ_S indicating the SR behavior. Parameters $M = 2000$, $\lambda_b = 0.6$, and $\lambda_d = 0.1$ are used.

we can see how much the extinction time alters due to the environmental change. For instance, along the path $\mathcal{T}_1$ shown in Fig. 3, MTE ratio of unperturbed case to perturbed case is given by $\exp(\epsilon S_p) \approx 0.5379$ for $\epsilon = 0.01$ and $\omega = 0.2$, which means that the external field makes MTE nearly cut in half.

To measure how much MTE is reduced due to the external field, we apply the linear response theory to MTE. This gives the measure so-called logarithmic susceptibility [4,30],

$$\chi_S(\omega, \mu) = \left|\lim_{\delta h \to 0} \frac{\delta \log \tau_E}{\delta h}\right| = |S_p|. \tag{21}$$

The logarithmic susceptibility χ_S evaluated along the extinction trajectory is shown in Fig. 4. As we expected from Sec. III, χ_S also has a peak at some finite value of μ at a given ω. Hence, we conclude that the SR behavior still remains for MTE.

V. SUMMARY AND DISCUSSION

We consider a coexisting two-species population under periodic environmental changes. By adding time-varying functions to the interspecific competition payoffs, we implement environmental changes and treat them as an external field h. Mainly, we analyze how the abundance fluctuations and the mean time to extinction respond against the external field and observe the stochastic resonance (SR) behavior by varying interspecific competition μ for both. The existence of SR peak indicates that neither too low nor too high interspecific competition payoffs μ make the system unstable to stay in the coexistence state.

We used an analogy between a Lyapunov function of the dynamical system and free-energy landscape, which leads us to interpret the interspecific interaction payoff μ as "temperature." Taking this analogy into account, we define susceptibilities using linear response theory: χ_D and χ_S for the abundance fluctuations and the mean time to extinction, respectively. Both measurements work well to detect SR peaks showing good agreement of the analogy.

Interestingly, the peak positions of susceptibilities χ_D and χ_S do not match. This discrepancy may come from the mea-

surement scale of each susceptibility: The χ_D measures how much the abundance fluctuates near the coexistence (a local quantity) while χ_S is calculated in the region from the coexistence to extinction (a global quantity). The relation between these local and global quantities is still a remaining question for future work.

ACKNOWLEDGMENTS

J.I.P. and B.J.K. were supported by the National Research Foundation of Korea (NRF) grant funded by the Korea government (MSIT) Grant No. 2019R1A2C2089463. H.J.P. was supported by the NRF grant funded by the Korea government (MSIT) Grant No. 2020R1A2C1101894 and by an appointment to the JRG Program at the APCTP through the Science and Technology Promotion Fund and Lottery Fund of the Korean Government. This work was also supported by the Korean Local Governments–Gyeongsangbuk-do Province and Pohang City.

APPENDIX A: LYAPUNOV FUNCTION

A Lyapunov function is a potential-like smooth scalar function that describes a dynamical system. More precisely, for a dynamical system $\dot{\mathbf{n}} = \mathbf{f}(\mathbf{n})$ with a set of fixed points $\{\mathbf{n}_i^*\}$, a Lyapunov function $\phi(\mathbf{n})$ is defined as follows: (i) $\dot{\phi}(\mathbf{n}) \leqslant 0$ for all $\mathbf{n}$ and (ii) $\dot{\phi}(\mathbf{n}) = 0$ if and only if $\mathbf{n} \in \{\mathbf{n}_i^*\}$. By definition, the certain path that minimizes the Lyapunov function represents the flow of the original system. This scalar function is much easier to handle than high-dimensional ODEs, yet obtaining the functional form of Lyapunov function needs "divine inspiration" [31].

Thankfully, one way for constructing the Lyapunov function of two-species Lotka-Volterra equation has been developed in Ref. [32]. Following the procedure in Ref. [32], we calculate the Lyapunov function of Eq. (5) with $h = 0$,

$$\phi(n, m) = \frac{\mu}{2M^2}(n^2 + m^2) - \frac{\lambda\mu}{M}(n + m) + \frac{nm}{M^2}. \tag{A1}$$

We can easily check that Eq. (A1) satisfies the two conditions in the definition. First, the time derivative of the Lyapunov function $\phi(n, m)$ is

$$\begin{aligned}\dot{\phi}(n, m) &= \frac{\partial\phi}{\partial n}\dot{n} + \frac{\partial\phi}{\partial m}\dot{m} \\ &= -\frac{n}{\mu M}\left(\frac{\mu}{M}n - \lambda\mu + \frac{m}{M}\right)^2 \\ &\quad - \frac{m}{\mu M}\left(\frac{\mu}{M}m - \lambda\mu + \frac{n}{M}\right)^2 \leqslant 0\end{aligned} \tag{A2}$$

for all $n, m \geqslant 0$. Second, the equality in Eq. (A2) holds only at $(n, m) = (0, 0),\ (\lambda M, 0),\ (0, \lambda M),\ (\frac{\mu}{\mu+1}\lambda M, \frac{\mu}{\mu+1}\lambda M)$ which exactly correspond to the fixed points of Eq. (5) with $h = 0$.

Using normalized variables $x = n/M$ and $y = m/M$, we now show that the curvature of Lyapunov function in Eq. (A1) near the coexistence state $\mathbf{x}^* = (\frac{\mu\lambda}{\mu+1}, \frac{\mu\lambda}{\mu+1})$ only depends on the interspecific interaction μ. Since $\phi_x(\mathbf{x}^*) = \phi_y(\mathbf{x}^*) = 0$ from $\dot{\phi}(\mathbf{x}^*) = 0$, where the subscripts denote the derivative with respect to the given parameter, the quadratic approximation of Eq. (A1) at $\mathbf{x}^*$ is

$$\begin{aligned}\phi(x, y)|_{\mathbf{x}^*} &= \frac{1}{2}\left[\phi_{xx}(\mathbf{x}^*)x^2 + 2\phi_{xy}(\mathbf{x}^*)xy + \phi_{yy}(\mathbf{x}^*)y^2\right] \\ &= \frac{1}{2}\left[\mu x^2 + 2xy + \mu y^2\right].\end{aligned} \tag{A3}$$

To eliminate the cross term of x and y, we define new variables $x_\parallel = (x - y)/\sqrt{2}$ and $x_\perp = (x + y)/\sqrt{2}$, and Eq. (A3) is now

$$\phi(x, y)|_{\mathbf{x}^*} = \frac{1}{2}\left[(\mu - 1)x_\parallel^2 + (\mu + 1)x_\perp^2\right], \tag{A4}$$

with the corresponding principal curvatures $k_\parallel = \mu - 1$ and $k_\perp = \mu + 1$ [33]. This suggests that the curvature depends only on μ. Furthermore, the direct relations between principal curvatures and relaxation times in Eq. (8) are $\tau_\parallel^{-1} = \frac{\lambda}{\mu+1}k_\parallel$ and $\tau_\perp^{-1} = \frac{\lambda}{\mu+1}k_\perp$.

APPENDIX B: ABUNDANCE FLUCTUATION AS THE AVERAGED LINEAR NOISE

Our model based on individual level stochastic processes represented in Eq. (1) which can be described by the master Eq. (14). It is well known that the dynamics of the averaged abundance $\langle n\rangle = \sum_{n,m} nP_{n,m}$ and $\langle m\rangle = \sum_{n,m} mP_{n,m}$ calculated from the master Eq. (14) is equivalent to the deterministic Eq. (5). The similar relation can be derived for the averaged abundance fluctuation $\langle\delta_x\rangle$ and $\langle\delta_y\rangle$ calculated from the master equation and the fluctuations in Eq. (7). Using the system size expansion technique developed by van Kampen [34], we show that the averaged abundance fluctuation around the stationary state with zero-field behaves in the same way with the fluctuations described in the deterministic Eq. (5).

In this approach, we rewrite the master equation using the raising and lowering operators $\mathbb{E}_n^{\pm1} : n \longmapsto n \pm 1$ and $\mathbb{E}_m^{\pm1} : m \longmapsto m \pm 1$,

$$\begin{aligned}\frac{d}{dt}P_{n,m}(t) &= \lambda_b\left[\left(\mathbb{E}_n^{-1} - 1\right)n + \left(\mathbb{E}_m^{-1} - 1\right)m\right]P_{n,m}(t) \\ &\quad + \lambda_d\left[\left(\mathbb{E}_n^{1} - 1\right)n + \left(\mathbb{E}_m^{1} - 1\right)m\right]P_{n,m}(t) \\ &\quad + \frac{1}{M}\left[\left(\mathbb{E}_n^{1} - 1\right)n(n-1) + \left(\mathbb{E}_m^{1} - 1\right)m(m-1)\right]P_{n,m}(t) \\ &\quad + \frac{1}{\mu M}\left[\left(\mathbb{E}_n^{1} + \mathbb{E}_m^{1} - 2\right)nm\right]P_{n,m}(t).\end{aligned} \tag{B1}$$

Because the probability distribution $P_{n,m}(t)$ has a sharp peak around the solution of Eq. (5), $n = M\bar{x}(t)$ and $m = M\bar{y}(t)$, with a width of order $\sqrt{M}$, we expand the abundances in terms of the system size factor M, $n = M\bar{x} + \sqrt{M}\xi$ and $m = M\bar{y} + \sqrt{M}\zeta$. We call ξ and ζ are linear noise variables. For given $\bar{x}(t)$ and $\bar{y}(t)$, n and m have one-to-one mapping to ξ and ζ, and thus a probability distribution $\Pi(\xi, \zeta, t)$ can replace $P_{n,m}(t)$.

Since the master equation is calculated with fixed n and m, the time derivation of $P_{n,m}(t)$ becomes

$$\begin{aligned}\frac{dP}{dt} &= \frac{\partial\Pi}{\partial t} + \frac{d\xi}{dt}\frac{\partial\Pi}{\partial\xi} + \frac{d\zeta}{dt}\frac{\partial\Pi}{\partial\zeta} \\ &= \frac{\partial\Pi}{\partial t} - \sqrt{M}\left(\frac{d\bar{x}}{dt}\frac{\partial\Pi}{\partial\xi} + \frac{d\bar{y}}{dt}\frac{\partial\Pi}{\partial\zeta}\right).\end{aligned} \tag{B2}$$

With the change of variables, the raising and lowering operators are transformed into $\mathbb{E}_\xi^{\pm1} : \xi \longmapsto \xi \pm M^{-1/2}$ and $\mathbb{E}_\zeta^{\pm1} : \zeta \longmapsto \zeta \pm M^{-1/2}$. Expanding the operators up to the order of M^{-1},

$$\mathbb{E}_\xi^{\pm1} = 1 \pm M^{-1/2}\frac{\partial}{\partial\xi} + M^{-1}\frac{\partial^2}{\partial\xi^2} + O(M^{-3/2}),$$
$$\mathbb{E}_\zeta^{\pm1} = 1 \pm M^{-1/2}\frac{\partial}{\partial\zeta} + M^{-1}\frac{\partial^2}{\partial\zeta^2} + O(M^{-3/2}), \quad \text{(B3)}$$

we can obtain

$$\begin{aligned}
&\frac{\partial\Pi}{\partial t} - \sqrt{M}\left(\frac{d\bar{x}}{dt}\frac{\partial\Pi}{\partial\xi} + \frac{d\bar{y}}{dt}\frac{\partial\Pi}{\partial\zeta}\right)\\
&= \lambda_b\left[-\sqrt{M}(\bar{x}\partial_\xi + \bar{y}\partial_\zeta) + \left(\bar{x}\partial_\xi^2 + \bar{y}\partial_\zeta^2\right) - (\partial_\xi\xi + \partial_\zeta\zeta)\right]\Pi\\
&+\lambda_d\left[\sqrt{M}(\bar{x}\partial_\xi + \bar{y}\partial_\zeta) + \left(\bar{x}\partial_\xi^2 + \bar{y}\partial_\zeta^2\right) + (\partial_\xi\xi + \partial_\zeta\zeta)\right]\Pi\\
&+\left[\sqrt{M}\left(\bar{x}^2\partial_\xi + \bar{y}^2\partial_\zeta\right) + \left(\bar{x}^2\partial_\xi^2 + \bar{y}^2\partial_\zeta^2\right) + 2(\bar{x}\partial_\xi\xi + \bar{y}\partial_\zeta\zeta)\right]\Pi\\
&+\frac{1}{\mu}\left[\sqrt{M}\bar{x}\bar{y}(\partial_\xi + \partial_\zeta) + \bar{x}\bar{y}\left(\partial_\xi^2 + \partial_\zeta^2\right) + (\partial_\xi + \partial_\zeta)(\bar{x}\zeta + \bar{y}\xi)\right]\Pi,
\end{aligned} \quad \text{(B4)}$$

with the notation $\partial_x = \frac{\partial}{\partial x}$. Comparing the terms with the order of $\sqrt{M}$, we get

$$\frac{d\bar{x}}{dt} = \lambda\bar{x} - \bar{x}^2 - \frac{1}{\mu}\bar{x}\bar{y},$$
$$\frac{d\bar{y}}{dt} = \lambda\bar{y} - \bar{y}^2 - \frac{1}{\mu}\bar{x}\bar{y}, \quad \text{(B5)}$$

which reproduces Eq. (5). Collecting the order of 1 gives us a form of linear multivariate Fokker-Planck equation

$$\frac{\partial\Pi}{\partial t} = -\sum_{i,j} A_{ij}\frac{\partial}{\partial\xi_i}(\xi_j\Pi) + \frac{1}{2}\sum_{i,j} B_{ij}\frac{\partial^2\Pi}{\partial\xi_i\partial\xi_j}, \quad \text{(B6)}$$

where $\xi_1 = \xi$ and $\xi_2 = \zeta$ with

$$\mathbf{A} = \begin{bmatrix} \lambda - 2\bar{x} - \bar{y}/\mu & -\bar{x}/\mu \\ -\bar{y}/\mu & \lambda - 2\bar{y} - \bar{x}/\mu \end{bmatrix},$$
$$\mathbf{B} = \begin{bmatrix} \bar{x}(\lambda_b + \lambda_d + \bar{x} + \bar{y}/\mu) & 0 \\ 0 & \bar{y}(\lambda_b + \lambda_d + \bar{y} + \bar{x}/\mu) \end{bmatrix}. \quad \text{(B7)}$$

From Eq. (B7), we can obtain the dynamics of ξ and ζ by multiplying the variable and taking average for it,

$$\frac{d}{dt}\langle\xi\rangle = \left(\lambda - 2\bar{x} - \frac{\bar{y}}{\mu}\right)\langle\xi\rangle - \frac{\bar{x}}{\mu}\langle\zeta\rangle,$$
$$\frac{d}{dt}\langle\zeta\rangle = -\frac{\bar{y}}{\mu}\langle\xi\rangle + \left(\lambda - 2\bar{y} - \frac{\bar{x}}{\mu}\right)\langle\zeta\rangle. \quad \text{(B8)}$$

Since we want to describe the averaged abundance fluctuations around the stationary state with zero field, $(\bar{x}^*, \bar{y}^*) = (\frac{\mu\lambda}{\mu+1}, \frac{\mu\lambda}{\mu+1})$, we define the fluctuations $\langle\delta_x\rangle \equiv \langle n - M\bar{x}^*\rangle/M$ and $\langle\delta_y\rangle \equiv \langle m - M\bar{y}^*\rangle/M$; that is to say $\langle\delta_x\rangle = \bar{x} - \bar{x}^* + \langle\xi\rangle/\sqrt{M}$ and $\langle\delta_y\rangle = \bar{y} - \bar{y}^* + \langle\zeta\rangle/\sqrt{M}$. At stationary state, thus combining Eq. (B5) and Eq. (B8) eventually gives

$$\frac{d}{dt}\langle\delta_x\rangle = -\frac{\mu\lambda}{\mu+1}\langle\delta_x\rangle - \frac{\lambda}{\mu+1}\langle\delta_y\rangle + O(M^{-1}),$$
$$\frac{d}{dt}\langle\delta_y\rangle = -\frac{\lambda}{\mu+1}\langle\delta_x\rangle - \frac{\mu\lambda}{\mu+1}\langle\delta_y\rangle + O(M^{-1}), \quad \text{(B9)}$$

which is equivalent to the dynamics of abundance fluctuation δ_x and δ_y in Eq. (7) with $h = 0$. It implies that the abundance fluctuation derived from the deterministic Eq. (5) reflects the stochastic effect.

With nonzero h, the additional term appears in Eq. (14), $-\frac{h}{\mu^2 M}[(\mathbb{E}_n^1 - \mathbb{E}_m^1)nm]P_{n,m}(t) + O(h^2)$ for small h. This additional term perturbs Eq. (B5) and Eq. (B8) as

$$\frac{d\bar{x}}{dt} = \lambda\bar{x} - \bar{x}^2 - \left(\frac{1}{\mu} - \frac{h}{\mu^2}\right)\bar{x}\bar{y},$$
$$\frac{d\bar{y}}{dt} = \lambda\bar{y} - \bar{y}^2 - \left(\frac{1}{\mu} + \frac{h}{\mu^2}\right)\bar{x}\bar{y}, \quad \text{(B10)}$$

and

$$\frac{d}{dt}\langle\xi\rangle = \left(\lambda - 2\bar{x} - \frac{\bar{y}}{\mu} + \frac{h}{\mu^2}\bar{y}\right)\langle\xi\rangle - \left(\frac{\bar{x}}{\mu} - \frac{h}{\mu^2}\bar{x}\right)\langle\zeta\rangle,$$
$$\frac{d}{dt}\langle\zeta\rangle = -\left(\frac{\bar{x}}{\mu} + \frac{h}{\mu^2}\bar{y}\right)\langle\xi\rangle + \left(\lambda - 2\bar{y} - \frac{\bar{x}}{\mu} - \frac{h}{\mu^2}\bar{x}\right)\langle\zeta\rangle, \quad \text{(B11)}$$

respectively. If $h \sim O(M^{-1/2})$, then we can finally obtain the averaged abundance fluctuation dynamics at $(\bar{x}^*, \bar{y}^*) = (\frac{\mu\lambda}{\mu+1}, \frac{\mu\lambda}{\mu+1})$,

$$\frac{d}{dt}\langle\delta_x\rangle = \frac{\lambda^2}{(\mu+1)^2}h - \frac{\mu\lambda}{\mu+1}\langle\delta_x\rangle - \frac{\lambda}{\mu+1}\langle\delta_y\rangle + O(M^{-1}),$$
$$\frac{d}{dt}\langle\delta_y\rangle = -\frac{\lambda^2}{(\mu+1)^2}h - \frac{\lambda}{\mu+1}\langle\delta_x\rangle - \frac{\mu\lambda}{\mu+1}\langle\delta_y\rangle + O(M^{-1}), \quad \text{(B12)}$$

which is equivalent to Eq. (7).

[1] C. J. Svensson, E. Johansson, and P. Åberg, J. Anim. Ecol. **75**, 765 (2006).

[2] E. S. Poloczanska, S. J. Hawkins, A. J. Southward, and M. T. Burrows, Ecology **89**, 3138 (2008).

[3] R. L. Kordas, C. D. G. Harley, and M. I. O'Connor, J. Exp. Mar. Biol. Ecol. **400**, 218 (2011).

[4] M. Assaf, A. Kamenev, and B. Meerson, Phys. Rev. E **78**, 041123 (2008).

[5] P. G. Hufton, Y. T. Lin, T. Galla, and A. J. McKane, Phys. Rev. E **93**, 052119 (2016).
[6] P. G. Hufton, Y. T. Lin, and T. Galla, Phys. Rev. E **99**, 032122 (2019).
[7] I. Meyer and N. M. Shnerb, Phys. Rev. Research **2**, 023308 (2020).
[8] C. Escudero, Phys. Rev. E **74**, 010103(R) (2006).
[9] L. Gammaitoni, P. Hänggi, P. Jung, and F. Marchesoni, Rev. Mod. Phys. **70**, 223 (1998).
[10] Z. Néda, Phys. Rev. E **51**, 5315 (1995).
[11] B. J. Kim, P. Minnhagen, H. J. Kim, M. Y. Choi, and G. S. Jeon, Europhys. Lett. **56**, 333 (2001).
[12] S. K. Baek and B. J. Kim, Phys. Rev. E **86**, 011132 (2012).
[13] H. J. Park, S. K. Baek, and B. J. Kim, Phys. Rev. E **89**, 032137 (2014).
[14] A. Gabel, B. Meerson, and S. Redner, Phys. Rev. E **87**, 010101(R) (2013).
[15] G. W. A. Constable and A. J. McKane, Phys. Rev. Lett. **114**, 038101 (2015).
[16] H. J. Park and A. Traulsen, Phys. Rev. E **96**, 042412 (2017).
[17] P. Czuppon and A. Traulsen, J. Math. Biol. **77**, 1233 (2018).
[18] S. Smale, J. Math. Biol. **3**, 5 (1976).
[19] M. L. Zeeman, Proc. Amer. Math. Soc. **123**, 87 (1995).
[20] W. Huang, C. Hauert, and A. Traulsen, Pro. Natl. Acad. Sci. USA **112**, 9064 (2015).
[21] M. Doi, J. Phys. A: Math. Gen. **9**, 1465 (1976).
[22] V. Elgart and A. Kamenev, Phys. Rev. E **70**, 041106 (2004).
[23] I. Lohmar and B. Meerson, Phys. Rev. E **84**, 051901 (2011).
[24] O. Gottesman and B. Meerson, Phys. Rev. E **85**, 021140 (2012).
[25] M. Assaf and B. Meerson, J. Phys. A: Math. Theor. **50**, 263001 (2017).
[26] C. Escudero and A. Kamenev, Phys. Rev. E **79**, 041149 (2009).
[27] M. Assaf and B. Meerson, Phys. Rev. E **81**, 021116 (2010).
[28] A. I. Chernykh and M. G. Stepanov, Phys. Rev. E **64**, 026306 (2001).
[29] T. Grafke, R. Grauer, and T. Schäfer, J. Phys. A: Math. Theor. **48**, 333001 (2015).
[30] V. N. Smelyanskiy, M. I. Dykman, H. Rabitz, and B. E. Vugmeister, Phys. Rev. Lett. **79**, 3113 (1997).
[31] S. H. Strogatz, *Nonlinear Dynamics and Chaos with Student Solutions Manual: With Applications to Physics, Biology, Chemistry, and Engineering* (CRC Press, Boca Raton, FL, 2018), p. 203.
[32] Y. Tang, R. Yuan, and Y. Ma, Phys. Rev. E **87**, 012708 (2013).
[33] B. O'neill, *Elementary Differential Geometry* (Academic Press, San Diego, CA, 2014), pp. 214–215.
[34] N. van Kampen, *Stochastic Processes in Physics and Chemistry* (North-Holland, Amsterdam, 2007), pp. 257–267.